current (veratridine< 0.5 umol/l) do not alter calcium and sodium handling in myocytes isolated from wild type mice.

Conclusion: The characteristics of sodium channel mutation can be mimicked with veratridine and TTX. Calcium and sodium handling is not different in ventricular myocytes isolated from wild type mice and mice carrying the 1795insD+ mutation.

3110-Pos Structure-function Relashionship Of Two Spider Toxins PnTx2-5 And PnTx2-6

Paulo S. L. Beirão[1], Alessandra Matavel[2], Cécile Fleury[1], Carlos H. Ramos[3], Franck Molina[4]

[1] *UFMG, Belo Horizonte, Brazil,*
[2] *Univ. Rochester, Rochester, NY, USA,*
[3] *UNICAMP, Campinas, Brazil,*
[4] *CNRS FRE 3009, Montpellier, France.*

Board B413

The venom of the Brazilian solitary spider *Phoneutria nigriventer* contains potent polypeptide neurotoxins. Among them, a family of similar toxins (Tx2 type) causes excitatory symptoms such as salivation, lachrymation, priapism, convulsions, spastic paralysis and death. The toxins PnTx2-5 and PnTx2-6 differ only in five of their 48 amino acids and have 10 cysteine residues forming 5 disulphide bridges. We took advantage of this difference to investigate structure-activity relationship. Both toxins inhibit sodium current inactivation of GH3 cells, similar to the alpha-scorpion toxins, except that PnTx2-6 is not displaced by high depolarizing pulses. Furthermore, they partially compete with alpha-scorpion toxins in binding assays [personal communication]. PnTx2-6 has 3 times higher affinity than PnTx2-5 ($K_{0.5}$ = 32nM and 95nM, respectively). Conventional homology modelling was not possible, because of low sequence similarity with other known structures. However, as all short spider toxins present the same overall fold, templates were chosen according to their cysteine pattern in the spider neurotoxin classification proposed by Kozlov *et al.* in 2005. The cysteine connectivity pattern has been deduced by sequence alignment with all cysteine-rich short spider toxins whose 3D structures have previously been experimentally determined and present the Inhibitory-Cysteine-Knot (ICK) motif. Finally, a three-dimensional model of each toxin structure was performed using Modeller package version 8v2. The models were successfully tested by several evaluation software. Fluorescence spectroscopy confirms the exposition of Phe36 and Circular Dicroism spectra confirms the absence of alpha-helix and presence of beta-sheet and beta-turns, as predicted by the models. The amino acid residues that differ in the toxins are predicted to be exposed. Our models suggest a key role of Phe36 and Tyr41 in the binding of both toxins to the channel, while Tyr35, Trp37 and Trp40 can account for the higher affinity of PnTx2-6.

Voltage-gated Ca Channels

3111-Pos Different Structure-function Relationships Determine Biophysical Properties And Pharmacological Modulation Of T-type Calcium Channels Cav3.1 And Cav3.2

Peter Bartels[1], Kerstin Behnke[1], Jung H. Lee[2], Paula Q. Barrett[3], Edward Perez-Reyes[3], Jan Matthes[1], Stefan Herzig[1]

[1] *University of Cologne, Cologne, Germany,*
[2] *Sogang University, Seoul, Democratic People's Republic of Korea,*
[3] *University of Virginia, Charlottesville, VA, USA.*

Board B414

The family of T-type calcium channels consists of three isoforms, respectively $Ca_V3.1$(α1G), $Ca_V3.2$(α1H) and $Ca_V3.3$(α1I). Whole-cell recordings allow for an only limited discrimination between T-type calcium channel isoforms. For that, we followed these goals, respectively:

1. Comparison of $Ca_V3.1$ (GGGG) and $Ca_V3.2$ (HHHH) by their single-channel gating properties.
2. Single-channel recording of chimera constructs, composed of N-terminal domains DI and DII of $Ca_V3.1$ and C-terminal domains DIII and DIV of $Ca_V3.2$, respectively (construct 1, GGHH) and (construct 2, HHGG) for structure-function analysis.
3. A detailed analysis of interaction between single $Ca_V3.1$ and $Ca_V3.2$ with N_2O that has previously been described as a $Ca_V3.2$-selective blocker at the whole-cell level (Todorovic et al., *Mol Pharmacol 60*:603–610, 2001).

In HEK-cells we find baseline activity of single $Ca_V3.1$ pore-subunits (n=6) to be significantly lower compared to $Ca_V3.2$ (n=7) (e.g. I_{peak}: −8.2±2.1 fA vs. −19.8±3.6 fA; P_{open}: 2.2±0.2% vs. 4.5±0.5%). Interestingly, gating properties of construct 2 (HHGG, n=6), mirror that of $Ca_V3.1$ (I_{peak}: −6.8±1.5; P_{open}: 2.3±0.2%), while gating properties of construct 1 (GGHH, n=8) are similar to that of $Ca_V3.2$ (I_{peak}: −15.2±2.5 fA; P_{open}: 4.3±0.3%). These findings indicate that baseline activity is mediated by the C-terminal two domains DIII and DIV. We find N_2O to inhibit both T-type calcium channel isoforms $Ca_V3.1$ and $Ca_V3.2$ in a potential-dependent manner, with more pronounced block of $Ca_V3.2$. Preliminary experiments with chimeric α1 subunits suggest that the $Ca_V3.1$-like chimera (HHGG) is more susceptible to N_2O blockade, thus pointing at N_2O effects to be mediated by N-terminal structures of T-type calcium channels.

3112-Pos Two Distinct α_{1S} Residues In Bony Fishes Incompatible With $Ca_V1.1$ Ca^{2+}-conductance

Johann Schredelseker, Manisha Shrivastav, Sandra Schleret, Manfred Grabner

Innsbruck Medical University, Innsbruck, Austria.

Board B415

Whole-cell patch clamp analysis of zebrafish primary skeletal myotubes revealed the presence of a non-Ca^{2+}-conducting $Ca_v1.1$ despite the existence of robust charge movement and intracellular Ca^{2+} transients. Studying chimeras between the Ca^{2+}-conducting α_{1S} from rabbit (rb-α_{1S}) and the non-conducting α_{1S} from zebrafish (zf-α_{1S}), we could identify an Asn to Asp substitution in homologous repeat II as relevant for this phenomenon. This Asp, three residues C-terminal to the selectivity filter Glu, was sufficient to eliminate Ca^{2+} currents in heterologous expression when introduced into rb-α_{1S}. The Asn to Asp exchange was also found in the likewise non-Ca^{2+}-conductive α_{1S} of the closely related carp. To test if a non-Ca^{2+}-conductive α_{1S} is an exclusive trait of zebrafish relatives, we patch clamped primary myotubes of the model organism Medaka as a distant representative from the class of bony fishes. Like in zebrafish, recordings from Medaka myotubes showed no Ca^{2+} inward currents. However, the Asn to Asp-substitution lacked in Medaka α_{1S}. In contrast, an exchange of charges (Asp to Lys) was identified in repeat I, four residues C-terminal to the selectivity filter Glu. The corresponding point-mutant rb-α_{1S}D396K was unable to restore L-type Ca^{2+} currents. Sequence analysis of selected bony fishes revealed either the Asn to Asp exchange in repeat II or the Asp to Lys exchange in repeat I in numerous species. Thus, in contrast to classes below (cartilaginous fishes) or beyond (tetrapoda), bony fishes seem to encounter an evolutionary pressure for a non-Ca^{2+}-conductive $Ca_v1.1$. Whether $Ca_v1.1$ non-conductivity evolved convergently by the two described mutations (analogous traits) or can be attributed to so far unidentified common mutations (homologous trait) will be evaluated.

Supported: FWF-DK-W1101-B12 & MFI 6180

3113-Pos Insights Into Interactions Between The Voltage-gated Ca2+ Channel Beta-subunit, RGK Proteins And Rim3 Protein Using FRET

Damian J. Williams, Henry L. Puhl III, Stephen R. Ikeda

NIAAA, Bethesda, MD, USA.

Board B416

RGK proteins and Rim proteins are different protein families that have recently been shown to modulate voltage-gated Ca^{2+} channel (VGCC) activity through interaction with the Ca^{2+} channel β-subunit ($Ca_v\beta$). The RGK family of Ras-related small GTPases comprises Rad, Gem/Kir, Rem1 and Rem2 proteins and function as potent inhibitors of VGCCs. The Rim family of proteins are expressed in the synapse, and Rim1 inhibits voltage-dependent inactivation of VGCCs. In this study, Förster resonance energy transfer (FRET) efficiency was used to investigate interactions between $Ca_v\beta3$ and RGK or Rim3 proteins. Cerulean fluorescent protein-tagged $Ca_v\beta3$ and venus fluorescent protein-tagged RGK proteins or Rim3 were expressed in HeLa cells. In live cells, FRET efficiencies between the tagged proteins were determined using 3-filter cube FRET fluorescence microscopy. Significant FRET occurred between $Ca_v\beta3$ and wild-type Rem2 or Gem. The FRET between $Ca_v\beta3$ and Gem was abolished when a $Ca_v\beta3$ mutant lacking the guanylate kinase (GK) domain was used. This result supports a role for the GK domain in RGK-$Ca_v\beta3$ association. Significant FRET occurred between $Ca_v\beta3$ and Rim3, a distinct member of the Rim protein family with high sequence homology to the C-terminus of Rim1. This result suggests an interaction between Rim3 and $Ca_v\beta3$, and a possible role for Rim3 in VGCC modulation.

3114-Pos Does Na^+ Preserve The Cardiac Ca^{2+} Channel Conductance During Hypoxia?

Shahrzad Movafagh, Martin Morad

Georgetown University Medical Center, Washington, DC, USA.

Board B417

Hypoxia is known to reduce cardiac L-type Ca^{2+} current. The mechanism of this inhibition is not fully understood although redox modification of both intra and extracellular channel motifs has been strongly implicated. Here we report a pronounced hypoxic suppression of cardiac Ca^{2+} current that is in part dependent on ionic concentration of extracellular Na^+. When rat cardiomyocytes were voltage clamped in hypoxic extracellular solutions containing either 140mM Na^+ or Li^+, baseline L-type current amplitude was suppressed by 10% within 60 seconds of exposure. However, when Na^+ was substituted with Cs^+ or TEA^+ reducing $[Na^+]_o$ to 10mmol/L, I_{Ca} was suppressed by about 50% over 15 seconds of hypoxia. Furthermore, the hypoxic suppression of I_{Ca} was not caused by a shift in steady state availability of Ca^{2+} channels and there was no significant change in the reversal potential of I_{Ca}. Taken together these data suggest a modulatory role of extracellular Na^+ on Ca^{2+} channel conductance under hypoxia. The finding that this modulation is seen in presence of Cs^+, TEA^+ and not Na^+ or Li^+ implies possible interaction of smaller alkali metals with the channel proteins in physiological ion concentrations. It is likely that such interactions are critical in preserving Ca^{2+} channel conductance under hypoxic conditions.

3115-Pos Developmental Expression and Localization of Cav1.3 L-type Ca Channel in Rat Heart

Yongxia S. Qu[1,2], Eddy Karnabi[1], Mohamed Chahine[3], Mohamed Boutjdir[1,2]

[1] *SUNY Downstate Medical Center, Brooklyn, NY, USA,*
[2] *VA New York Harbor Healthcare system, Brooklyn, NY, USA,*
[3] *Hôpital Laval, Research Center,, Quebec, QC, Canada.*

Board B418

Background and aim: neuron-endocrine α_{1D} L-type Ca channel (Cav1.3) has been recently identified in *adult* supraventricular tissue and plays critical roles in sinoatrial function. Our goal is to characterize the differential expression and localization of α_{1D} Ca channel during heart development.

Methods and Results: Western blot using rat cardiac tissue at different developmental stages (fetal, neonatal and adult) showed that protein level of α_{1D} Ca channel is about 9 fold higher in fetal compared to adult stage. At fetal and neonatal stages, two forms of α_{1D} Ca channel were observed: a full size (250 kD), and a short form (190 kD) with the full size being predominant. In the adult heart, only atrial tissue expressed the short form α_{1D} Ca channel, while the ventricular tissue did not reveal any detectable α_{1D} Ca channel proteins. Confocal images were consistent with the Western blot findings and showed α_{1D} Ca channel in both atrial and ventricular myocytes at fetal and neonatal stages, but not in adult ventricular cells. Interestingly, bright nuclear staining in addition to the sarcolemmal staining was observed in fetal/neonatal myocytes but not in adult atrial cells.

In conclusion, the data show abundant expression of α_{1D} Ca channel in the immature heart and distinct localization compared to adult heart. These observations suggest that α_{1D} Ca channel may play a more important role in excitation-coupling of the immature heart where the sarcoplasmic reticulum is less developed.

3116-Pos Effects Of Sequence Differences And Cellular Environment On Calcium-dependent Inactivation Of $Ca_V1.2$ And $Ca_V1.1$ Calcium Channels

Joshua D. Ohrtman[1], Symeon Papadopoulos[2], Barbara Ritter[2], Kurt G. Beam[1]

[1] *University of Colorado Health Sciences Center, Aurora, CO, USA,*
[2] *Medical University Hannover, Hannover, Germany.*

Board B419

An interaction between CaM and the "IQ" motif in the C-terminus of $Ca_V1.2$ has been implicated in calcium-dependent inactivation (CDI) of the channel. Despite considerable conservation, the IQ motif of $Ca_V1.1$ differs at several residues, including ^{1532}H and ^{1537}M, from $Ca_V1.2$ (^{1658}Y, ^{1663}K). Previously, we showed that the mutations Y>H and K>M reduce the CaM binding ability of C-terminal fragments of $Ca_V1.2$. Here we have examined the effects of introducing these mutations into full-length $Ca_V1.2$ on CDI after expression in tsA-201 cells together with β_{2a} and $\alpha_2\delta$-1. For wt $Ca_V1.2$, the fraction of current remaining 50 ms after the peak inward current (R_{50}) displayed a U-shaped dependence on test potential with Ca as charge carrier, mirroring the peak I–V relationship; R_{50} for wt $Ca_V1.2$ had little voltage-dependence between +10 and +60 mV with Ba as charge carrier. By contrast, R_{50} for (Y>H/K>M)-$Ca_V1.2$ had a voltage-dependence in Ca that was not U-shaped and similar to that of R_{50} in Ba. With the eventual goal of determining how the reciprocal mutations (H>Y/M>K) affect the function of $Ca_V1.1$ in a muscle cell, we expressed wt $Ca_V1.2$ in dysgenic myotubes which are null for endogenous $Ca_V1.1$. Unlike either tsA-201 cells or native cardiac cells, $Ca_V1.2$ in dysgenic myotubes did not display CDI, suggesting the possibility that CDI is actively inhibited by the cellular environment within skeletal muscle. We are currently attempting to identify the reason that $Ca_V1.2$ lacks CDI in a skeletal muscle environment.

Supported by NIH NS24444 and AR44750 to K.G.B.

3117-Pos Molecular and Functional Mechanisms of PKA Phosphorylation of α_{1D} L-type Calcium Channel

Omar Ramadan[1], Yongxia Qu[1], Raj Wadgaonkar[1], Ghayath Baroudi[2], Mohamed Chahine[3], Mohamed Boutjdir[1,4]

[1] *Molecular and Cellular Cardiology Program, VA New York Harbor Healthcare System & SUNY Downstate Medical Center, Brooklyn, NY, USA,*
[2] *Department of Pharmacology, Faculty of Medicine, Université de Montréal, Montréal, QC, Canada,*
[3] *Le Centre de Recherche Université Laval Robert-Giffard and Department of Medicine, Laval University, Quebec, QC, Canada,*
[4] *NYU School of Medicine, New York, NY, USA.*

Board B420

Background: α_{1D} L-type Ca channel is exclusively expressed in the supraventricular tissue and has been implicated in the pacemaker activity of the heart and atrial fibrillation. We recently demonstrated that α_{1D} Ca channel is regulated by protein kinase A (PKA) pathway which in turn regulates the pacemaker activity. Accordingly, we hypothesized that PKA regulation of α_{1D} Ca channel is mediated through phosphorylation of specific consensus sites on the C-terminus of α_{1D} Ca channel.

Methods and Results: GST fusion proteins of the proximal and distal C-terminus of α_{1D} Ca channel were generated. In vitro PKA kinase assay of GST fusion proteins of the C-terminus of α_{1D} Ca channel was performed. The in vitro PKA kinase assay was followed by Western blotting using PhosphoDetect™ anti-PKA substrate and anti-phosphoserine antibodies. The proximal part of the C-terminus of α_{1D} Ca channel was phosphorylated. The distal part of the C-terminus of α_{1D} Ca channel was minimally phosphorylated. Serine 1816 and serine 1743 on the proximal C-terminus of α_{1D} Ca channel were found to be phosphorylated by Mass Spectrometry. Site directed mutagenesis and patch clamp studies showed that serine 1816 and serine 1743 were major functional phosphorylation sites for PKA.

Conclusion: Biochemical and functional data show that serine 1816 and serine 1743 on the proximal C-terminus of α_{1D} Ca channel are major functional PKA phosphorylation sites for PKA. These novel findings provide new insights in the PKA regulation of α_{1D} Ca channel in the normal heart and in atrial fibrillation.

3118-Pos Magnesium Block in CaV 3.1

Katie C. Bittner, Dorothy A. Hanck

University of Chicago, Chicago, IL, USA.

Board B421

Mg^{2+}, an important physiological cation, present in mM concentrations both inside and outside mammalian cells, is well known to block divalent and monovalent cation permeation in L-type Ca^{2+} channels. Although it has been well studied, there remain some inconsistencies in the data as to whether Mg^{2+} only voltage dependently blocks or whether it can also permeate ("punch through"). For T-type Ca^{2+} channels, the data are more limited in that only $[Mg^{2+}]_o$ has been examined, i.e. it has been described using either a one or

two site blocking model with a very high barrier to the cytoplasm. The aim of this study was to understand the interactions of both $[Mg^{2+}]_o$ and $[Mg^{2+}]_i$ with the T-type Ca^{2+} channel, $Ca_V3.1$, that affect monovalent permeation.

Under conditions of symmetrical Li^+, both $[Mg^{2+}]_i$ and $[Mg^{2+}]_o$ voltage dependently blocked Li^+ currents. At more extreme potentials block was voltage-dependently relieved, as would be expected for "punch through" of Mg^{2+} ions. Consistent with this idea, we could record inward Mg^{2+} currents in the presence of 20mM $[Mg^{2+}]_o$ and the impermeant monovalent cation $[TEA^+]_o$ (120 mM) and 140 mM $[Li^+]_i$. Both $[Mg^{2+}]_o$ and $[Mg^{2+}]_i$ effects were well described by a model of permeant block, in which in the absence of a voltage gradient $[Mg^{2+}]_o$ had a 100-fold higher affinity than $[Mg^{2+}]_i$, 0.33±0.03mM (n=7) compared to 41±5mM (n=12). The electrical distance for $[Mg^{2+}]_o$ block was 0.44±0.01 from the outside and for $[Mg^{2+}]_i$ was 0.50±0.03 from the inside. The very large difference in affinity between $[Mg^{2+}]_o$ and $[Mg^{2+}]_i$ points to asymmetry along the permeation pathway which could reflect multiple binding sites and/or differences in accessibility secondary to Mg^{2+} dehydration.

Supported by F31-NS058334 (K.B.) and RO1-HL065680 (D.H.)

3119-Pos Biophysical Characterization Of Rat Cardiac Cav3.2 T-type Calcium Channel Alternative Splice Variants

Laurence S. David, Esperanza Garcia, Elana M. Thau, Stuart M. Cain, John R. Tyson, Terrance P. Snutch

University of British Columbia, Vancouver, BC, Canada.

Board B422

The Cav3.2 T-type calcium channel plays important roles in cardiac pacemaking and cardiovascular physiopathology. Alternative splicing of Cav3.2 generates functional diversity. Using full length cDNA generated from rat cardiac tissue, we have systematically identified alternative splice variants of Cav3.2 calcium channels. Here we report the biophysical analysis of splice variants located in the III–IV linker [Cav3.2 (+ exon 25) and Cav3.2 (− exon 25)] and their corresponding C-terminus splice variant [(Cav3.2(−25/35a) and Cav3.2(+25/35a)]. The III–IV linker is subjected to alternative splicing (+/− exon 25) whereas the C-terminus is spliced to create a truncated channel by generating an alternative stop (35a). In cardiac tissue from newborn rats we find an ~ 95% transcripts of Cav3.2 isoforms lacking exon 25. Biophysical analysis of the Cav3.2 channels (+25) and (−25) expressed in HEK cells using whole cell patch clamp recording shows differences in voltage-dependent gating properties and current kinetics. We find an ~5 mV leftward shift in voltage-dependence of activation in variants expressing exon 25 (−47.64 ± 0.43) compared to splice variants without exon 25 (−42.57 ± 0.45). The (−25) exon variant channels also recover faster and to a level more than 100% compared with (+25) variant channels. In terms of kinetics, Cav3.2 (−25) channels exhibit slower time-to-peak and slower inactivation rate compared with Cav3.2 (+25) channels, whereas (−25) channels deactivate faster than (+25) channels. We find voltage-dependent facilitation is significantly more pronounced in (−25) variants than (+25) variant channels. Currently, we are exploring the mechanism of this facilitation as well as the contribution of the (35a) C-terminal splice variants towards Cav3.2 functional alterations. Our findings demonstrate that alternative splicing confers functionally distinct biophysical properties on Cav3.2 T-type calcium channels.

3120-Pos Downregulation of the L-type Ca^{2+} Channel by Pharmacological Preconditioning in Mammalian Heart

German Gonzalez, Daniel Zaldivar, Elba D. Carrillo, Maria C. Garcia, Jorge A. Sanchez

Cinvestav, Mexico, D.F., Mexico.

Board B423

Ischemic preconditioning (IP) is a physiological phenomenon in which a brief period of ischemia activates endogenous mechanisms that protect cardiomyocytes from a subsequent prolonged ischemia. IP can be mimicked by pharmacological agents like diazoxide, an opener of mitochondrial K_{ATP} channels. Although action potentials are shortened by IP, the possibility that cardiac Ca^{2+} channels are regulated by IP has not been explored. Our present experiments test this possibility.

Methods: Isolated rat hearts were preconditioned by diazoxide (100 μM). $Ca_{V1.2}$ channel currents were measured in isolated cardiomyocytes using the whole cell patch-clamp technique. By differential centrifugation, the ventricle membrane fraction was obtained and used in Western blots.

Results: We found that Ca^{2+} channel currents have a peak of −10±1.1 (n=70) pA.pF^{-1} under control conditions and −3.0±0.1 (n=10) pA.pF^{-1} in the presence of diazoxide. No shifts in the I–V relation were observed. The possibility that the current amplitude reduction is mediated by PKC (a well known mediator of IP) was explored next. PKC was blocked by the potent and selective PKC inhibitor, chelerythrine, for 30' and diazoxide was tested after PKC inhibition. The reduction in current amplitude was not prevented by chelerythrine, indicating that it is not mediated by PKC. We then explored the possibility of downregulation of $Ca_{V1.2}$ channels at the protein level by diazoxide. Antibodies raised against the α_{1c} subunit, the principal subunit of $Ca_{V1.2}$ channels, revealed a drastic reduction in the protein content of membrane α_{1c}. This reduction is consistent with the physiological data and suggests that the L-type channel in heart is downregulated during ischemic preconditioning.

Supported in part by CONACYT Grant # 60880.

3121-Pos Modulation Of L-type Ca Channels By The Distal C-terminal Of $Ca_V1.4$: Simultaneous Effects On Ca^{2+}-dependent Inactivation And Voltage-dependent Activation

Xiao-dong Liu, Philemon S. Yang, David T. Yue

Johns Hopkins University, Baltimore, MD, USA.

Board B424

Ca^{2+}-dependent inactivation (CDI) and voltage-dependent activation are two major characteristics of Ca_V channel function, which are oft viewed as separate processes. For example, coexpressing Ca_V channels with wild-type calmodulin (CaM_{WT}) versus a Ca^{2+}-insensitive mutant (CaM_{1234}) respectively permits and eliminates CDI, yet produces little or no differences in activation (Yang *et al*, *J Neurosci* ***26***:10677). However, in the case of $Ca_V1.4$, a customized channel restricted to retinal neurons, recent experiments suggest that these two processes may be intimately linked (Singh *et al*, *Nat Neurosci* ***9***:1108). In these channels, the distal C-terminal domain (ICDI) not only eliminates CDI, but positively shifts the half-activation voltage $V_{1/2}$. To test whether the dual effect of ICDI generalizes beyond $Ca_V1.4$, we constructed chimeric channels wherein the distal C-terminal domain of $Ca_V1.4$ was fused onto $Ca_V1.2$ and $Ca_V1.3$ channels, which are more ubiquitous members of the L-type channel family. By contrast to previous reports, fusing variable segments of the $Ca_V1.4$ C-terminal domain did not appreciably affect the voltage-dependent inactivation of chimeric channels (Singh *et al*, *Nat Neurosci* ***9***:1108; Wahl-Schott *et al*, *PNAS* ***103***:15657). Nonetheless, these variable fusions did yield graded decreases in CDI, and different positive shifts in $V_{1/2}$. Interestingly, the extent of these two effects was quantitatively correlated in both $Ca_V1.2$ and $Ca_V1.3$ contexts. These results support the notion that CDI and activation may be mechanistically linked across L-type calcium channels. This may prove to be an interesting theme, as little is currently known about how CaM/channel binding is transduced into CDI.

3122-Pos Role of Protein Kinase A (PKA) in the Dopaminergic Regulation of $Ca_v3.2$ Channels

Changlong Hu, Seth D. DePuy, Junlan Yao, Paula Q. Barrett

University of Virginia, Charlottesville, VA, USA.

Board B425

Dopamine plays an important role in determining fluid and electrolyte balance, and abnormalities in its production or function produces hypertension. Among its major actions is the inhibition of aldosterone synthesis from cells of the adrenal zona glomerulosa (ZG), a multi-step process that depends on the activity of low-voltage-activated (LVA), $Ca_v3.2$ Ca channels. Although it is well established that dopamine inhibits LVA channel activity in many tissues via a mechanism that depends on Gβγ dimers, the role of cAMP signaling in Gβγ-mediated $Ca_v3.2$ channel inhibition remains controversial.

We recorded whole cell and single channel Ca currents from cultured model ZG cells (H295R) expressing wild-type and mutant $Ca_v3.2$ channels. Dopamine inhibited whole cell current dose dependently (1–50μM) at all voltages (50μM: 20.3±1.7%, n=16), changing neither the voltage-dependence of activation nor inactivation. Overexpression of Gβγ scavengers: Gα-transducin or β-adrenergic receptor kinase C-terminus, abrogated channel inhibition (5.6±2.2%, n=16). Surprisingly, at all doses dopamine-induced channel inhibition was augmented significantly with 10 μM 8Br-cAMP and precluded by the inclusion of a PKA inhibitor (PKI, 10μM) in the patch pipette. Mutation of a single PKA consensus site within the channel II–III loop that selectively binds β_2 containing Gβγ dimers also prevented channel inhibition (7.2±2.1%, n=7), suggesting further a permissive role for PKA activity in $G\beta_2\gamma_x$-mediated inhibition of $Ca_v3.2$ channels. Accordingly, the selective inhibition of $Ca_v3.2$ unitary currents recorded from inside-out membrane patches by recombinant $G\beta_2\gamma_2$ dimers required both cellular pretreatment with 8Br-cAMP and a wild-type channel. Neither mutant $Ca_v3.2$ channels nor recombinant $G\beta_1\gamma_2$ dimers permitted modulation. We conclude that dopamine inhibition of $Ca_v3.2$ channels is both PKA- and $G\beta_2$-dependent, and establish a permissive role for cAMP in the Gβγ regulation of $Ca_v3.2$ channels.

3123-Pos Gating of Single $Ca_V1.3$ Channels Expressed in Hek293 Cells

Hye Kyung Lee, Eun Mi Lee, Seung Whan Kim, Young-Hoon Kim, Hae Won Kim

University of Ulsan College of Medicine, Seoul, Republic of Korea.

Board B426

L-type Ca^{2+} channel subtype $Ca_V1.3$ has been suggested to be important in many neuronal and non-neuronal cell functions. In the present study we characterized gating properties of single $Ca_V1.3$ channels transiently expressed in HEK293 cells. The cells were transfected with a mixture of cDNAs (kindly provided by Dr. Lipscombe from the Brown University) encoding α_1D, β_3 and $\alpha_2\delta$ and the cell-attached mode of patch clamp technique was employed using 100 mM Ba^{2+} as a charge carrier. Throughout the study 1 μM Bay K8644 was present in the bath solution. Preliminary results indicate that slope conductance of $Ca_V1.3$ was 28 ± 2 pS (n=18). The open dwell times were fit by two exponentials with the mean open time constants of 0.5 and 5.1 ms at +20mV, which did not vary with the test potential. Shut time histograms were also fit by two exponentials. The brief shut time component (τ_{sh1}=0.4 ms, +20 mV) did not vary with the test potential, while the longer shut time (τ_{sh2}) component decreased with voltage from 12ms at −20 mV to 3 ms to +20 mV. Mean open probability (measured over 100 ms) increased with depolarization, although there was a large variation within each voltage. The gating properties of single $Ca_V1.3$ are compared to those of native $Ca_V1.2$ recorded from rat ventricular myocytes.

(This study was supported partly by a grant (2003-316) from the Asan Institute for Life Sciences, Seoul, Korea.)

3124-Pos Congenital Heart Block: Antigenicity of the Extracellular Loop (Domain I, S5–S6) of α1D L-type Ca Channel

Eddy Karnabi[1], Yongxia Qu[1], Raj Wadgaonkar[1], Salvatore Mancarella[1], Yunkun Yue[2], Mohamed Chahine[3], Robert Clancy[4], Jill Buyon[4], Mohamed Boutjdir[1,4]

[1] *Molecular and Cellular Cardiology Program, VA New York Harbor Healthcare System & SUNY Downstate Medical Center, Brooklyn, NY, USA,*
[2] *Molecular and Cellular Cardiology Program, VA New York Harbor Healthcare System, Brooklyn, NY, USA,*
[3] *Le Centre de Recherche Universite Laval Robert-Giffard and Department of Medicine, Laval University, Quebec, QC, Canada,*
[4] *NYU School of Medicine, New York, NY, USA.*

Board B427

*Background*_AutoImmune-associated congenital heart block (CHB) is established as a passively acquired autoimmune disease in which transplacental passage of autoantibodies against intracellular ribonucleoproteins SSB/La(48kDa), and SSA/Ro(52kD and 60kD) results in damage to the developing fetal heart. The hallmark of CHB is complete atrioventricular block. Our group has shown that anti-Ro/La autoantibodies inhibit alpha 1D L-type Ca current ($I_{Ca\text{-}L}$) and cross-react with the alpha 1D Ca channel protein. This study aims at identifying the possible binding sites on alpha 1D protein for anti-Ro/La autoantibodies, specifically the extra-cellular regions in Domain I, II, III, and IV S5–S6 P-Loops.

*Methods and Results*_GST fusion proteins of the extracellular regions (S5–S6) of each of the four domains I–IV were prepared and tested for reactivity with sera from mothers with CHB children using enzyme-linked immunosorbent assay (ELISA). Fifty five CHB sera and 28 control healthy sera from the Research Registry for Neonatal Lupus were used in this study. Serum samples from 8 of 55 (14.5%) mothers with a child with CHB reacted with the extracellular loop E1 corresponding to Domain I S5–S6 region. In contrast, only 2 of 28 (7.1%) healthy control sera reacted with the E1 loop. Electrophysiological characterization of the anti-alpha 1D positive CHB-sera revealed inhibition of alpha 1D L-type Ca current ($I_{Ca\text{-}L}$) (44.1%) in tsA201 transfected cells.

*Conclusion*_These results demonstrate that the extra-cellular loop Domain I S5–S6 of alpha 1D Ca Channel is an antigenic target of pathological autoantibodies in CHB. Although these autoantibodies are less prevalent than anti-Ro/La autoantibodies, the presence of such reactivity suggests an additional risk factor in the pathogenesis of CHB.

3125-Pos Gamma6-Subunit Modulates Gating and Pharmacology of T-Type Calcium Channels

Katja Witschas, Jan Matthes, Stefan Herzig, Elza Kuzmenkina

University of Cologne, Cologne, Germany.

Board B428

High-voltage-activated calcium channels are multimeric protein complexes. However, the subunit composition of low-voltage-activated (T-type) calcium channels is not yet resolved. A recombinant pore-forming $alpha_1$-subunit alone appears to reproduce all functional properties of native T-type calcium channels. Auxiliary beta- and $alpha_2$delta-subunits were found to augment surface expression of T-type calcium channels. A role of gamma-subunits is unclear. Recently, $gamma_6$-subunits were identified to uniquely inhibit ion currents through T-type $Ca_v3.1$ channels (Hansen *et al.*, J Mol Cell Cardiol 2004;*37*:1147–58). The question remained whether some channels become entirely non-functional due to an effect of $gamma_6$-subunits or $gamma_6$-subunits associate with $Ca_v3.1$ channels changing their biophysical properties. Here, we present patch-clamp measurements performed at single-channel resolution. Our data demonstrate that $gamma_{6L}$-subunit significantly reduces availability of the channels by trapping them for a longer time in the blank state. We also observed that the average activity of $Ca_v3.1$ channels expressed in HEK-293 cells slowly fluctuated on the timescale of tens of minutes. Intriguingly, $gamma_{6L}$-subunit mostly affected channel availability within the more-active state. As a negative control we used $gamma_7$-subunit, which indeed produced no effect on the channel gating.

Furthermore, the pharmacological properties of $Ca_v3.1$ channels were also modulated by $gamma_{6L}$-subunit. The selective T-type calcium antagonist mibefradil was used to probe channel pharmacology. Our data support the concept of two mibefradil binding sites with different affinities and blocking mechanisms (*cf.* Michels *et al.*, Mol Pharmacol 2002;*61*:682–94). Co-expression of $gamma_{6L}$-subunit resulted in ten-fold decrease of the apparent affinity for mibefradil. This agrees with the concept that mibefradil binds to open and inactivated states, since $gamma_{6L}$-subunit reduces the probability of the channel to open.

In conclusion, $gamma_{6L}$-subunits are capable of fine-tuning the activity of expressed T-type calcium channel pores, in agreement with other known "silencing" functions of gamma-subunits.

3126-Pos Trace Metals (Zn^{2+} and Cu^{2+}) Are Essential Modulators Of Recombinant $Ca_V2.3$ Calcium Channels

Aleksandr Shcheglovitov, Edward Perez-Reyes

University of Virginia, Charlottesville, VA, USA.

Board B429

It is believed that calcium influx through $Ca_v2.3$ calcium channels affects a great diversity of functions in the CNS including fear memory formation, pain perception, and synaptic plasticity. However, the pharmacological profile of these channels is still a matter of debate. Here we investigated the sensitivity of these channels towards the physiologically important metals Zn^{2+} and Cu^{2+}. Our findings suggest that these cations influence the gating and conductance of $Ca_v2.3$ channels differently. In the voltage range between -40 mV to 15 mV, these channels were highly sensitive to extracellular Zn^{2+} and Cu^{2+} concentrations (IC_{50} ~ 600 and 0.8 nM correspondingly). However, the effect of these cations gradually diminished with further depolarization (IC_{50} ~ 5.2 μM and 0.2 μM at +20 mV for Zn^{2+} and Cu^{2+}, respectively). Based on the finding that $Ca_v3.2$ channels also contain a high affinity binding site for Zn^{2+} and Cu^{2+}, and that a histidine (H191) in the IS3–S4 loop is involved in this binding, we hypothesized that similarly located residues in $Ca_v2.3$ (H179 and H183) may be mediating metal block. Indeed, mutations of these residues markedly reduce (by up to 6-fold) the trace metal affinity of these channels at negative voltages. Additionally, we discovered that Zn^{2+} and Cu^{2+} affect current kinetics differently, which provides a "signature" of the interaction of these ions with $Ca_v2.3$ channels. Overall, our data indicate that the most abundant transition metals in the CNS, zinc and copper, are potent

modulators of $Ca_v2.3$ calcium channels, even at submicromolar, physiologically relevant, concentrations, and the effects of these cations on channel gaiting mostly rely on the extracellular molecular determinant with two crucial histidines at its core.

3127-Pos Competition between Beta-subunits of Cardiac L-type Calcium Channels at Single Channel Level

Wanchana Jangsangthong[1], Ramin Akhavan-Malyer[1], Elza Kuzmenkina[1], Jan Matthes[1], Roger Hullin[2], Stefan Herzig[1]

[1] *University of Cologne, Cologne, Germany,*
[2] *Inselspital Bern, Bern, Switzerland.*

Board B430

Cardiac L-type calcium channels are composed of a pore forming $alpha_1$ and auxiliary beta- and $alpha_2$delta-subunits. Beta-subunits chaperone channels to the plasma membrane and modulate their gating. Beta-subunits are markedly different in modulation of biophysical channel properties. Thus, investigating single-channel gating gives opportunity to monitor a hypothesized alternation of different beta-subunits within the channel complex. We focused on two dominant cardiac beta-subunit isoforms

1. $beta_{1a}$-subunits, that produce moderate stimulation of channel gating and
2. $beta_{2b}$-subunits, that cause high channel activity and appear to be involved in heart failure. We characterized gating of single channels co-expressed in HEK-293 cells with either $beta_{1a}$ or $beta_{2b}$ or with both, $beta_{1a}$ and $beta_{2b}$-subunits, respectively.

When co-expressing both beta-subunits, gating switched between low-activity ($beta_1$-like) and high-activity ($beta_2$-like) modes on a minute time-scale (Figure A). Simultaneous examination of gating parameters of any individual sweep leads to a visual distinction between activity modes within each experiment (Fig B–D). Our results indicate a model of mutually exclusive binding and effective competition between beta-subunits.

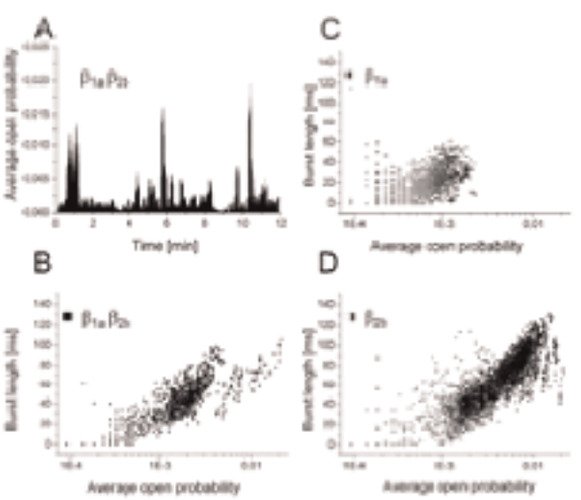

3128-Pos Cross-talk Between the Three α1C sites of modulation of $Ca_v1.2$ calcium channels by $Ca_v\beta_2$ subunits

Evgeny Kobrinsky, Qi Zong Lao, Sam Thomas, Jo Beth Harry, Nikolai M. Soldatov

National Institute on Aging, NIH, Baltimore, MD, USA.

Board B431

Facilitation of the $Ca_v1.2$ calcium channel voltage gating by accessory $Ca_v\beta$ subunits requires their stable binding to the AID site and dynamic interaction with the IQ motif of the pore-forming α1C subunit. Additionally, in $Ca_v\beta_2$ we identified a 41-amino acid C-terminal essential determinant (β_2CED) that binds to the LA-IQ region in a Ca^{2+}/CaM-independent manner and stimulates Ca^{2+} currents in the absence of $Ca_v\beta$ subunits, but does not support Ca^{2+}-dependent inactivation (CDI). Because this MAGUK-independent regulation of $Ca_v1.2$ channels may be a potential pharmaceutical target, we studied effects of β_2CED on $Ca_v1.2$ channels containing different $Ca_v\beta$ subunits (β_{2d}, $\beta_{2d}\Delta$CED, β_{1b}, and β_3). β_2CED affected kinetics of inactivation and voltage-dependence of I_{Ca} of all these channels. However, only the β_3 subset (vascular and cardiac) of channels was deprived of CDI, indicating that β_2CED targets this property more selectively. To better characterize this modulation, we studied FRET between different $Ca_v\beta$ and/or β_2CED N-terminally labeled with monomeric variants of Venus (^{v}) and Cerulean (^{c}). FRET between $^{v}\beta_3$ and $^{c}\beta_3$ or $^{c}\beta_2$ CED (2 sites) but not between $^{v}\beta_{2d}$ and $^{c}\beta_{2d}$ or $^{c}\beta_2$CED (3 sites) was eliminated on inactivation of one of the common binding sites by substitution for alanines of 4 key amino acids of AID. Thus, three $Ca_v\beta$ binding sites may be simultaneously occupied by two rather than one $Ca_v\beta$. The selectivity of modulation of calcium channels containing $Ca_v\beta$ subunits by β_2CED depends on both the availability of its binding site (as with β_3) and specific molecular properties of $Ca_v\beta$.

Supported by the NIA Intramural Research Program.

3129-Pos Mn^{2+} Blocks, Permeates, And Shifts Gating Of $Ca_V3.1$ T-type Calcium Channels

Quentin Jamieson, Carlos A. Obejero-Paz, Stephen W. Jones

Case Western Reserve University, Cleveland, OH, USA.

Board B432

Mn^{2+} is a cofactor for enzymes, but can be neurotoxic at high concentrations. We have examined the effects of Mn^{2+} on $Ca_V3.1$ (α1G) channels, using whole-cell recording from stably transfected HEK 293 cells. Currents through maximally activated channels (measured from instantaneous I–V relationships) were reduced by addition of 1 mM Mn^{2+}, in a weakly voltage-dependent manner. With 2 mM $Ca^{2+}{}_o$, the apparent K_D for Mn^{2+} block was 2.3 mM at 0 mV, acting at an apparent electrical distance $\delta = 0.07$; with 2 mM $Ba^{2+}{}_o$, $K_D = 0.7$ mM, $\delta = 0.09$. However, higher concentrations of Mn^{2+} did not inhibit currents as strongly as expected from a Woodhull model. Replacement of Ca^{2+} with 2–10 mM Mn^{2+} demonstrated Mn^{2+} permeation: I_{Mn}/I_{Ca} ~0.15 from 10 to 150 mV

(at 2 mM). Outward currents (carried by Na^+) were reduced more strongly by Mn^{2+} than by Ca^{2+} or Ba^{2+}, but reversal potentials indicate Ca^{2+} selectivity ($P_{Mn}/P_{Ca} \sim 0.2$). Mn^{2+} also shifted channel activation to more positive voltages, by 27 ± 1 mV at 10 mM Mn^{2+} (in 2 mM Ca^{2+}, n=8). Previous results indicate that Ca^{2+}, Ba^{2+}, and Mg^{2+} shift gating of $Ca_V3.1$ as expected for a surface charge density of 1 e^-/98 $Å^2$; effects of Mn^{2+} are stronger, requiring also binding to the surface charge (K_D = 11 M) in terms of Gouy-Chapman-Stern theory. Overall, effects of Mn^{2+} on $Ca_V3.1$ closely resemble Fe^{2+}, except that inward currents are larger with Mn^{2+}. $Ca_V3.1$ is a possible pathway for entry of 'trace' metals into neurons and other cells.

3130-Pos Kinetics of calcium channel activation

Stanislav Beyl, Michaela Kudrnac, Annette Hohaus, Evgeny Timin, Steffen Hering

Department of Pharmacology and Toxicology, University of Vienna, Vienna, Austria.

Board B433

Voltage-gated Ca^{2+} channels ($Ca_v1.2$) were expressed in HEK 293 (tsA-201) cells and barium currents recorded in 5 mM $BaCl_2$ at 22–25°C using the patch-clamp technique. Steady state and kinetic characteristics of currents were described in frame of the paradigm that the mutations in IIS6 segment affect solely the stability of the pore without disturbing the voltage sensing machinery. In order to quantify the pore stability we estimated the rate constants of pore opening (α) and closure (β). Voltage dependent rate constants *x* and *y* described "unlocking" of the pore (transition from a resting state R to a state A - non conducting but ready to open). The rate constants of pore opening (α) and closure (β) were voltage independent. All IIS6 mutations (e.g. I781T, I781P, I781G, I781V, I781N, A782P, L779G, A780G etc) affected α and β without changing *x* and *y*. Our data demonstrate that the IIS6 mutations destabilizing the closed state (by increasing α) simultaneously stabilize the open state (decrease β). The rate constants of opening (α) in mutant channels display a significant reverse correlation ($r = -0.87 \pm 0.14$, $p<0.009$) with changes in hydrophobicity whereas rate constants of channel closure (β) revealed less significant positive correlation ($r = 0.76 \pm 0.19$, $p<0.04$) with changes in hydrophobicity. We conclude that hydrophobic interactions (most likely between S6 segments) stabilize the closed conformation of $Ca_v1.2$.

Supported by FWF P19614-B11.

3131-Pos A Flagellar Waveform Conversion Mutant of *Chlamydomonas* is Defective in the Expression of a Flagellar Calcium Channel

Gene Kenta Fujiu[1], Masahiro Sokabe[1,2], Kenjiro Yoshimura[1,3]

[1] *ICORP/SORST, Cell-Mechanosensing, JST, Nagoya, Japan,*
[2] *Dept. Physiol., Nagoya Univ. Grad. Sch. Med., Nagoya, Japan,*
[3] *Struc. Biosci., Grad. Sch. Life Environ. Sci. Univ Tsukuba, Tsukuba, Japan.*

Board B434

When *Chlamydomonas* cells are stimulated by intense light, they show photophobic response, in which the cells transiently swim backward. During the response, the flagella undergo a waveform conversion from an asymmetrical type to a symmetrical type. This change in the flagellar bending pattern has been assumed to be brought about by the Ca^{2+} influx into the flagella but the molecular entity has been unknown. *Chlamydomonas* mutants *ppr*1, *ppr*2, *ppr*3, and *ppr*4 are defective in showing the photophobic response. The defect is due to the loss of the ability to generate all-or-none Ca^{2+} current in the flagella [Matsuda et al., Cell Motil. Cytoskel. *41*: 353–362 (1998)]. We found that these mutants were also defective in the flagellar waveform conversion during the mechanoresponse. To the end of identifying the gene deficient in these mutants, we cloned partial cDNA sequences of the putative voltage dependent Ca^{2+} channels and examined their expression in *ppr* mutants. RT-PCR showed that *ppr*2 did not express one of the Ca^{2+} channel that was putatively named as calcium channel like gene in flagella (CLF). Isolation of the full length cDNA of CLF indicated that at least two splice variants were expressed. Longer cDNA encoded a gene similar to voltage gated Ca^{2+} channel. Quantitative PCR analysis showed that the expression of CLF was increased up to 3.6 folds during flagellar regeneration. The antibody raised against the cytoplasmic region between the domain II and III recognized a 200kDa polypeptide in the flagella. Immunofluorescent staining with anti- CLF antibody showed that the CLF was localized along the flagella with high density at the tip. We infer that CLF is a voltage gated Ca^{2+} channel responsible for the flagellar waveform conversion.

3132-Pos Mechanism of Spatial Ca^{2+} Selectivity within Nanometers of a Ca^{2+} Source

Michael R. Tadross, Ivy E. Dick, David T. Yue

Johns Hopkins Univ, Baltimore, MD, USA.

Board B435

Ca^{2+} sensors are commonly positioned within nanometers of Ca^{2+} sources to enable privileged Ca^{2+} signaling. Yet, such close Ca^{2+} source proximity would seemingly challenge a sensor's ability to integrate Ca^{2+} signals from distant sources, which is essential for coordinated signaling. A prototype for this configuration is the Ca^{2+} sensor calmodulin (CaM) in complex with Ca_V1–2 Ca^{2+} channels. A single CaM persistently associates with channels, and Ca^{2+} binding to its C- and N-lobes trigger different regulatory processes on the host channel. Though the lobes of CaM are separated by 6 nm, and thereby face the same Ca^{2+}, they remarkably favor spatially distinct Ca^{2+} sources: the C-lobe prefers intense intermittent Ca^{2+} influx via the host channel (local selectivity), whereas the N-lobe responds selectivity to diminutive persistent Ca^{2+} signals from distant sources (global selectivity). Here we reveal the mechanisms of these notable selectivities. Local selectivity is achieved by responding preferentially to Ca^{2+} intensity. By contrast, global selectivity is accomplished by decoding temporal features of nanodomain Ca^{2+} via a novel mechanism which favors Ca^{2+} persistence over intensity. This

mechanism is governed by several key parameters, including channel open probability, the speed of Ca^{2+} (un)binding from CaM, and the balance between channel affinity for Ca^{2+}/CaM versus apoCaM. We experimentally manipulate all three parameters, enabling exhaustive validation of the proposed mechanism. Open probability is controlled via a novel 'voltage-block' technique combined with channels engineered for enhanced opening. The speed of Ca^{2+} release from CaM is tested via characterization of C-lobe regulation (slow Ca^{2+} release) and N-lobe regulation (rapid Ca^{2+} release). Finally, the ratio of channel affinity for Ca^{2+}/CaM versus apoCaM is graded via mutagenesis of the *NSCaTE* Ca^{2+}/CaM binding site. In all, these findings and approaches promise generalization to many spatiotemporally selective Ca^{2+} decoding systems.

3133-Pos An Asynchronous Calcium-dependent Current Conducted by Cav2.1 and Cav2.2 Channels: Implications for Asynchronous Neurotransmitter Release

Alexandra P. Few, Todd Scheuer, William A. Catterall

University of Washington, Seattle, WA, USA.

Board B436

We have identified a Ca-dependent current that is observed for $Ca_V2.1$ or $Ca_V2.2$ channels, which conduct P/Q-type and N-type Ca^{2+} currents that initiate neurotransmitter release at conventional synapses, but is not observed for $Ca_V1.2$ channels, which conduct L-type Ca current. We measured Ca^{2+} currents in tsA-201 cells transfected with $Ca_V2.1$ or $Ca_V2.2$ channels containing β_{2a} subunits. Prolonged Ca^{2+} entry activates a Ca^{2+} current, I_{Asynch}, that is observed upon repolarization and decays slowly at the holding potential ($\tau \cong 200$ ms). $Ca_V1.2$ channels transfected in these cells conduct peak Ca^{2+} currents of similar size but I_{Asynch} is not observed. During trains of repetitive depolarizations, I_{Asynch} increases in a pulse-wise manner, providing Ca^{2+} entry that persists between depolarizations. I_{Asynch} correlates with global rises in intracellular Ca^{2+} as it is blocked by barium substitution and by 10 mM EGTA in the patch pipette. However, detection of this rise in intracellular Ca^{2+} does not require calmodulin (CaM), as mutations that prevent Ca^{2+} binding to CaM do not block I_{Asynch}. Similarly, mutations in the IQ-like motif and CaM binding domain in the carboxy-terminus of $Ca_V2.1$ that prevent CaM-binding do not block I_{Asynch}. The rise of I_{Asynch} during trains of impulses and the kinetics of decay of I_{Asynch} following repolarization resemble the rise and decay asynchronous neurotransmitter release at conventional synapses, suggesting that I_{Asynch} is a potential Ca^{2+} source for asynchronous neurotransmitter release.

This work was supported by R01 NSC022625 to WAC and F31 MH078345 to APF.

3134-Pos Dominant-Negative Effects of Episodic Ataxia Type 2 Mutations Involve Disruption of Membrane Trafficking of Human P/Q-type Ca^{2+} Channels

Chung-Jiuan Jeng[1], Min-Chen Sun[2], Yi-Wen Chen[2], Chih-Yung Tang[2]

[1] *Institute of Anatomy & Cell Biology, College of Medicine, National Yang-Ming University, Taipei, Taiwan,*

[2] *Dept of Physiology, College of Medicine, National Taiwan University, Taipei, Taiwan.*

Board B437

Episodic ataxia type 2 (EA2) is an autosomal dominant neurological disorder associated with mutations in the gene encoding pore-forming α_{1A} subunits of human P/Q-type calcium ($Ca_V2.1$) channels. The exact mechanism of how mutant channels cause such clinical EA2 features as cerebellar dysfunctions, however, remains unclear. Our previous functional studies in *Xenopus* oocytes support the idea that EA2 mutants may exert prominent dominant-negative effects on wild-type $Ca_V2.1$ channels. To further pursue the mechanism underlying this dominant-negative effect, we examined the effects of EA2 mutants on the subcellular localization pattern of GFP-tagged wild-type $Ca_V2.1$ channels in HEK293T cells. In the presence of EA2 mutants, wild-type channels displayed a significant deficiency in membrane targeting and a concurrent increase in cytoplasm retention. Moreover, the cytoplasmic fraction of wild-type channels co-localized with an endoplasmic reticulum (ER) marker, suggesting that a significant amount of wild-type $Ca_V2.1$ channels was trapped in the ER. This EA2 mutant-induced ER retention pattern was reversed by lowering the cell incubation temperature from 37 to 27 °C. We also inspected the effects of untagged EA2 mutants on the functional expression of GFP-tagged wild-type $Ca_V2.1$ channels in HEK293T cells. Whole-cell current density of wild-type channels was diminished in the presence of EA2 mutants, which was also reversed by 27-°C incubation. Finally, biochemical analyses indicated that EA2 mutants did not significantly affect the protein expression level of wild-type channels. Taken together, our data suggest that EA2 mutants induce significant ER retention of their wild-type counterparts, thereby suppressing the functional expression of $Ca_V2.1$ channels.

3135-Pos Pentobarbital Inhibition of Recombinant Human P/Q-type Voltage-gated Ca^{2+} Channels

Andrew Schober, Kevin Gingrich

NYU School of Medicine, New York, NY, USA.

Board B438

INTRODUCTION: Presynaptic P/Q-type voltage-gated Ca^{2+} channels (PQCCs) mediate excitatory neurotransmission. Therefore, PQCCs appear attractive potential targets of pentobarbital-triggered depression of the central nervous system. However, clinically

relevant concentrations (50μM) produce little inhibition (<7%) of rodent cerebellar PQCCs[1] arguing against involvement in anesthetic action. Recently, PQCC closure by inactivation was shown to depend critically on global cytosolic Ca^{2+} concentration[2]. In light of these observations, we re-examined pentobarbital (PB) action using human (α_{1A}) recombinant PQCCs and physiological cytosolic Ca^{2+} concentration.

METHODS: HEK-293 cells were cotransfected with cDNAs encoding human α_{1A} (pore-forming subunit), rabbit β_{2a} and α_2/δ subunits. Ca^{2+} currents (I_{Ca}) were measured using whole-cell patch-clamp (holding potential = −90mV). Bath (mM): TEA-OH,125; methanesulfonic acid,125; HEPES,10; and $CaCl_2$,10; pH 7.4 with TEA-OH. Pipette (mM): Cs-methanesulfonate,135; CsCl,5; $MgCl_2$,1; Mg-ATP,4; and HEPES,10; EGTA,0.5 (free $[Ca^{2+}] \cong$ 100nM); pH to 7.40 with CsOH. Cells were constantly superfused by either control or PB solutions.

RESULTS: Depolarizations (+10mV, 800ms) triggered characteristic I_{Ca} timecourse (initial increase reaching a peak followed by decay). PB (50μM) reversibly reduced peak I_{Ca} (32% ± 4.4% SEM, N=5), accelerated current decay, and depressed current at end-pulse (r800) (20% ± 2.2% SEM, N=5). These effects were concentration dependent.

CONCLUSION: PB produced significant inhibition of human PQCCs at therapeutic concentrations through peak current reduction and enhanced inactivation. The results point to a potential role of PB depression of PQCCs and associated excitatory synaptic transmission in the mechanism of barbiturate anesthesia. The marked sensitivity of human PQCCs to PB inhibition relative to rodent may arise from differences in species or free cytosolic Ca^{2+}.

References

(1). Hall et al., Anesthesiology *81*, 1994;
(2). Liang et al., Neuron *39*, 2003.

3136-Pos Modulation of Voltage-Gated Ca^{2+} Channels by Phosphatidylinositol 4,5-Bisphosphate and G Protein-Coupled Receptors

Byung Chang Suh, Bertil Hille

University of Washington, Seattle, WA, USA.

Board B439

We studied modulation of voltage-gated Ca^{2+} channels (VGCCs) in tsA cells transfected with L-type ($Ca_v1.3$) and N-type ($Ca_v2.2$) Ca^{2+} channels and M_1 or M_2 muscarinic receptors and/or various enzymes. Both channels are known to be regulated by G protein-coupled receptors via the Ca^{2+}/calmodulin and G protein βγ subunits, respectively. However, the modulation of Ca^{2+} channels by membrane phospholipids is less understood. We find that N- and L-type channels are inhibited by depletion of phosphatidylinositol 4,5-bisphosphate (PIP_2) from the plasma membrane. Using a rapamycin-induced translocatable polyphosphoinositide 5-phosphatase system to deplete PIP_2 inhibits N-type and L-type Ca^{2+} channels by ~45% and ~20%, respectively, without changes in voltage-dependence of gating. Current inhibition by this system is irreversible and slower than that by activating phospholipase C with the M_1 receptor agonist oxotremorine-M (Oxo-M). The Oxo-M-induced inhibition of N-type channels is insensitive to expression of IP_3 5-phosphatase, which cleaves IP_3 and prevents release of Ca^{2+} from intracellular stores, and to expression of RGS2, which blocks $G\alpha_q$-mediated signaling. However, L-type channel inhibition was almost completely blocked by these treatments. When the chelator of G protein βγ subunits β-ARKct was expressed, the inhibition of N-type, but not L-type, channels by M_1 receptor stimulation was strongly blocked. Thus βγ subunits are involved in inhibition of current in M_1-receptor-mediated channel inhibition. Pertussis toxin treatment completely blocked M_2 receptor-mediated N-type channel inhibition, whereas it did not affect M_1 receptor responses, suggesting that βγ subunits significantly contribute to N-type channel inhibition by G_q protein-coupled receptors. Together, our results show that PIP_2 is an important regulator of Ca^{2+} channel function and suggest that the βγ subunit is also involved in N-type channel regulation even when M_1 muscarinic receptors are activated.

Support: NIH grants NS08174 & AR17803

3137-Pos Modulation Of $Ca_V3.2$ Channels By Receptor To Neurokinines Type-1

Azahel J. Rangel, Ulises Meza

Universidad Autonoma de San Luis Potosi, San Luis Potosi, Mexico.

Board B440

Recent immunochemistry studies and electrophysiological registries from lamina I have shown that the implied nociceptive pathway are inhibited by antagonists of receptors to neurokinines type-1 (NK1). Also, it has been observed that this pathway can be attenuated by blocking of voltage-gated Ca^{2+} channels. On the other hand, molecular evidence exists of which channels Ca^{2+} which they are expressed predominantly in this region of the central nervous system correspond to $Ca_V3.2$ type. Whit base in these antecedents, we are exploring the possible functional interaction between receptors NK1 and $Ca_V3.2$ channels. Our experimental strategy includes the expression of receptor NK1 and $Ca_V3.2$ channels in cells HEK-293, and the later registry of the electrical activity of these last ones by means of the technique of patch-clamp in its configuration of whole-cell, using to the Ca^{2+} like carried of charger (10 mM), Under these conditions, we observed an inhibiting effect of neurokinine A (NKA; 10nM), a peptide agonist of receptor NK1, on the activity of $Ca_V3.2$ channels (inhibition = 22.6± 2.7%; n=6). The inhibiting action of NKA is independent of the voltage, it does no modify kinetic of activation and the inactivation of $Ca_V3.2$ currents, and is partially reversible. Interestingly, the inhibiting effect of NKA is attenuated by the RGS2 expression, a molecular kidnapper of the subunits Gαq/11 (inhibition = 15.2 ± 2.9%; n= 7) as well as by the previous application of PMA (200 nM), a well-known activator protein kinase C (PKC), (inhibition = 14.2 ± 1.8%; n= 8). Our results contribute preliminary evidence of possible modulation of the $Ca_V3.2$ channels by PKC through the activation of receptor NK1 by signalling to Gαq/11 proteins.

3138-Pos Inhibition of L-type Ca^{2+} Channel Currents by Epiandrosterone in Bovine Coronary Smooth Muscle Cells

Rikuo Ochi, Sachin A. Gupte

New York Medical College, Valhalla, NY, USA.

Board B441

L-type Ca^{2+} channel current ($I_{Ca,L}$) plays a key role in the regulation of blood flow by inducing contraction of vascular smooth muscle cells (VSMC). Naturally existing epiandrosterone (EPI), an inhibitor of glucose-6-phosphodehydrogenase (G6PD) that is a primary regulator of cellular redox by converting $NADP^+$ to NADPH, causes relaxation of high K^+-induced contraction of VSMC. We have shown that EPI inhibits $I_{Ca,L}$ in cardiac myocytes. We characterized $I_{Ca,L}$ as I_{Ba} from freshly isolated bovine coronary artery smooth muscle cells by whole-cell ruptured patch technique in the presence of 10 mM Ba^{2+} and clarified its modulation by EPI. I-V relationship of I_{Ba} was bell-shaped with peak amplitude of 5 pA/pF. I_{Ba} was remarkably augmented by BAY K8644. The voltage for 50 % inactivation ($V_{0.5}$) in a quasi-steady-state inactivation curve by 2 s pre-pulse was -25 mV. I_{Ba} during 2 s pulse decayed with the sum of two exponential curves. Ramp depolarization with a slope of 5 mV/s or staircase change of membrane potential with steps of 10 s revealed the presence of window I_{Ba} of 10% of the maximal current density with the peak at -15 mV. EPI dose-dependently and reversibly inhibited I_{Ba}: 100 μM EPI decreased peak current density by 30%, shifted $V_{0.5}$ by 8 mV to a negative direction, accelerated the time course of decay during depolarization and decreased the window current by 60%. The reduction of window current could be a mechanism of EPI-induced relaxation of high-K^+-induced contraction of VSMC. 6-aminonicotinamide, another G6PD blocker, also shifted $V_{0.5}$ to a negative direction and accelerated I_{Ba} decay during depolarization. These results support the hypothesis that the cellular redox is involved in the regulation of VSMC contraction by modulating $I_{Ca,L}$.

3139-Pos Ca2+-dependent Modulation of Cav1.1 via Calmodulin

Michelle Harline, Katarina Stroffekova

Utah State University, Logan, UT, USA.

Board B442

(CaM) has been documented for most high-voltage-activated Ca^{2+} channels, but whether the skeletal muscle L-type channel ($Ca_v1.1$) exhibits this property has been unknown. We shown previously by whole-cell current recordings of $Ca_v1.1$ currents obtained from cultured mouse myotubes that the fraction of current remaining at the end of the pulse displayed classic signs of Ca^{2+}-dependent inactivation (CDI), including U-shaped voltage dependence, maximal inactivation (~30%) at potentials eliciting maximal inward current, and virtual elimination of inactivation when Ba^{2+} replaced external Ca^{2+} or when 10 mM BAPTA was included in the pipette solution. Furthermore, CDI was virtually eliminated in normal myotubes overexpressing mutant CaM (CaM_{1234}) that does not bind Ca^{2+}, whereas CDI was unaltered in myotubes overexpressing wild-type CaM (CaM_{wt}).

In this paper, whole-cell current and fluorescent resonance energy transfer (FRET) recordings were obtained from cultured mouse myotubes to test which lobe of CaM is responsible for CDI of $Ca_v1.1$, and whether CaM associates with $Ca_v1.1$. A significant FRET signal (E=4.06%) was detected between fluorescently tagged $Ca_v1.1$ and CaM_{wt} coexpressed in dysgenic myotubes, demonstrating for the first time that these two proteins associate *in vivo*.

Supported by MDA (KS).

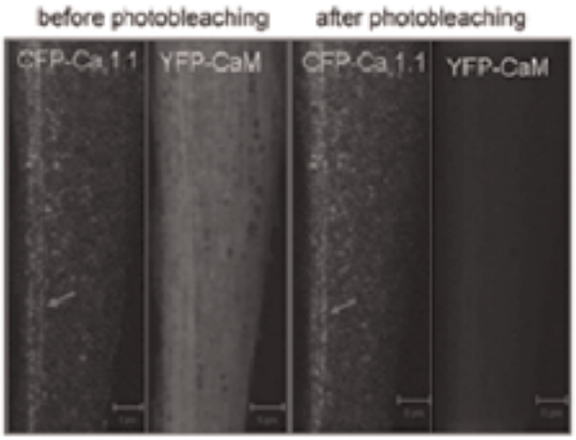

3140-Pos Cone-Shaped Lysophospholipids Modulate Voltage-Gated Calcium Channel Currents in Pituitary Cells

Galia Ben-Zeev, Itzhak Nussinovitch

Hebrew-University, Jerusalem, Israel.

Board B443

Lysophospholipids (LPLs) are lipophilic molecules consisting of a hydrophilic head and a hydrophobic tail. LPLs containing a large hydrophilic head and a thin hydrophobic tail were defined as cones. It was hypothesized that incorporation of cones into the outer leaflet of the phospholipid bilayer increases membrane tension and it was demonstrated that cone-shaped LPLs alter the gating of mechanosensitive ion channels. Previous studies demonstrated modulation of voltage-gated calcium channels (VGCC) by membrane stretch. We therefore examined the effects of the cone-shaped molecule, Lysophosphatidylchloline (LPC), on VGCC in pituitary cells. Our findings may be summarized as follows:

1. LPC (10–30 microM) differentially suppressed L-type and T-type calcium-channel currents (I_L and I_T, respectively); the effects on I_T were faster and more prominent than the effects on I_L.
2. The effects of LPC on I_L started after long delays (50–100s), exhibited slow onset kinetics and were reversible only after washout with BSA.

3. The effects of LPC on I_L were both dose-dependent and voltage-dependent with a rightward voltage shift of about 9 mV.
4. The effects of LPC on I_L persisted after block of G-proteins with GDPβS and after block of PKC with GF 109203X.
5. The effects of LPC on I_L were mimicked by lysophosphatidylinositol (LPI), a negatively charged cone-shaped lipophilic molecule.
6. The effects of LPC on I_L were not mimicked by a short chain LPC (C6:0) and by phosphatidylcholine, a cylindrical-shaped lipophilic molecule.

In summary, our results show that cone-shaped lipophilic molecules (LPC and LPI) suppress VGCC in pituitary cells and that this suppression is independent on the polarity of the hydrophilic head. Our results also suggest that incorporation of LPC and LPI into the phospholipid bilayer underlies this suppression, and that molecular shape is a determinant in this suppression.

3141-Pos The N-type (CaV2.2) Calcium Channel Domain III Contains The Tri-Substituted Purine (TSP)-Agonist Binding Site

Viktor Yarotskyy, Lei Du, Blaise Z. Peterson, Keith S. Elmslie

Penn State College of Medicine, Hershey, PA, USA.

Board B444

Roscovitine, a tri-substituted purine (TSP), possesses both agonist and antagonist effects on N-type (CaV2.2) calcium channels. The agonist effect is expressed as a slowed deactivation, which increases action potential-induced calcium influx leading to enhanced synaptic transmission. Roscovitine is the only known agonist for CaV2 channels and the site of action has yet to be determined. Identification of the TSP-agonist binding site has high scientific significance and potential clinical relevance. The first step was to determine the channel subunit that contained the agonist binding site. The roscovitine-agonist effect was not dependent on co-expression of the CaVα2δ subunit and was not altered by substituting the CaVβ1b subunit with β3. Based on this and other evidence we conclude that roscovitine binds to the α1B subunit to induce slowed deactivation. We have previously shown that L-type (CaV1.2) calcium channels lack the agonist response to roscovitine, which formed the basis for further experiments to identify the relevant N-channel domain. Chimeric channels were generated by moving either 1 or 2 domains from the N-type to the L-type channel, and each chimera was exposed to roscovitine to determine responsiveness. Roscovitine slowed deactivation of the LLNN (L-type domains I and II - N-type domains III and IV) chimera, which localized the agonist-binding site to domains III or IV. The effect was further isolated to domain III, since the LLNL chimera showed the agonist effect while roscovitine failed to alter deactivation of the LLLN chimera. We conclude, that the N-channel TSP-agonist binding site is located within domain III. Further localization of this binding site will highlight novel channel structures that regulate the gating of these neuron-specific calcium channels.

3142-Pos Modulation of Cardiac L-type $Ca_V1.2$ Calcium Channels by Phospholemman

Xianming Wang, Guofeng Gao, Blaise Z. Peterson

Penn State College of Medicine, Hershey, PA, USA.

Board B445

Ca^{2+} entry through L-type Ca^{2+} channels plays a critical role in shaping the action potential. Here, we report that cardiac Ca^{2+} channels are directly modulated by phospholemman (PLM), a single transmembrane protein that is important for regulating ion homeostasis in the heart through its interactions with the Na,K-ATPase and Na/Ca Exchanger. Experiments using confocal microscopy indiate that PLM and the calcium channel alpha-1 subunit, $Ca_V1.2$, co-localize to the plasma membranes of HEK293 and COS-7 cells. Recipricol co-immunoprecipitation studies demonstrate that PLM and $Ca_V1.2$ are specifically associated in the mouse heart and HEK 293 cells expressing the two proteins. Patch-clamp was used to assess the functional consequences of the interaction between PLM and the $Ca_V1.2$ subunit using HEK293 cells transfected with PLM or empty PLM vector. These studies demonstrate that PLM substantially slows the activation kinetics of $Ca_V1.2$ channels, but has no effect on neuronal $Ca_V2.1$ Ca^{2+} channels (not shown). As a result, Ca^{2+} entry during the first 50 msec of channel activation is decreased by up to 32%. Since PLM is upregulated in post-ischemic rat hearts, we propose that PLM-induced slowing of channel activation reduces peak $[Ca^{2+}]_i$ in infacted myocytes.

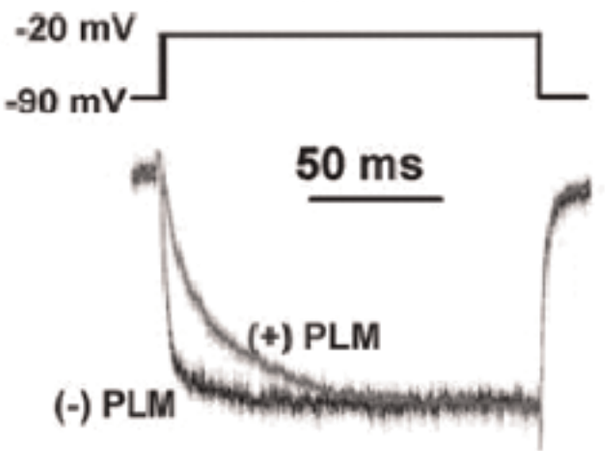

3143-Pos Caveolar Localization of $Ca_V1.2$ Channels Requires Association of $Ca_Vβ$ Subunit with Caveolin-3 in the Heart

Ravi C. Balijepalli, Jason D. Foell, Jabe M. Best, Timothy J. Kamp

University of Wisconsin, Madison, Madison, WI, USA.

Board B446

The auxiliary $Ca_V\beta$ subunits ($Ca_V\beta_1$-$Ca_V\beta_4$) regulate the trafficking and functional properties of the pore forming α subunit of $Ca_V1.2$ channels. Previously we have shown that a subpopulation of the $Ca_V1.2$ channels is localized to caveolae in ventricular myocytes. We hypothesize that caveolar localization of $Ca_V1.2$ channels requires specific $Ca_v\beta$ subunit isoform association with Caveolin-3 (Cav-3). Immnunoprecipitation using anti-Cav-3 and protein pull-down analysis with GST-Cav-3 detected associated $Ca_V\beta_2$ but not $Ca_V\beta_1$, $Ca_V\beta_3$, or $Ca_V\beta_4$ from mouse ventricular lysates. The impact of Cav-3 association with $Ca_V\beta$ on $I_{Ca,L}$ was analysed by the patch clamp technique in HEK293 cells. We used a dominant negative mutation of Cav-3 (P104L) associated with limb girdle muscular dystrophy to block plasma membrane expression of Cav-3 and associated proteins. Co-expression of P104LCav-3 with $Ca_V1.2$ alone in HEK293 cells did not affect current density or kinetics of $I_{Ca,L}$ compared to WT-Cav-3 co-expression. However, co-expression of P104LCav-3 with $Ca_V1.2$ and $Ca_v\beta_{2c,N4}$ significantly reduced $I_{Ca,L}$ density (~80%), resulted in a −5.7 mV shift in the voltage dependence of activation, and reduced the rate of $I_{Ca,L}$ decay compared to WT-Cav-3 co-expression. Subcellular localization of $Ca_v1.2$ channels was evaluated by immunocytochemistry using cells transfected with $Ca_v1.2$, Cav-3 or P104LCav-3 in presence and absence of $Ca_v\beta_{2c,N4}$ co-expression. Cells co-transfected with $Ca_v\beta_{2c,N4}$ and Cav-3, showed significant co-localization of $Ca_v1.2$ and Cav-3 at the plasma membrane. In contrast, $Ca_v\beta_{2c,N4}$+P104LCav-3 expression resulted in large intracellular inclusions containing both P104LCav-3 and $Ca_v1.2$, with minimal surface membrane expression of $Ca_v1.2$. However, in the absence of $Ca_v\beta_{2c,N4}$, $Ca_v1.2$ localization was comparable with Cav-3 and P104L Cav-3 coexpression. These findings suggest $Ca_v\beta_2$ subunit associates with Cav-3, and its expression is necessary for caveolar localization of $Ca_V1.2$ channels.

3144-Pos A New Splice Variant of the Skeletal Muscle Calcium Channel Reveals Distinct Gating Properties

Petronel Tuluc[1]

Natalia.A Molenda[2], Bettina Schlick[1], Gerald J. Obermair[1], Karin Jurkat-Rott[2], Bernhard E. Flucher[1]

[1] *Department of Physiology and Medical Physics, Innsbruck Medical University, Innsbruck, Austria,*
[2] *Department of Applied Physiology, Ulm, Germany.*

Board B447

The Ca^{2+} channel α_{1S} subunit (CaV1.1) is the voltage sensor of skeletal muscle excitation-contraction (EC) coupling. Upon membrane depolarization it rapidly triggers Ca^{2+} release from internal stores and itself conducts Ca^{2+}. However, this current is small, activates slowly and is not essential for skeletal muscle EC coupling. Here we identified a splice variant of the CaV1.1 α_{1S} subunit. In the human *CACNA1S* gene it lacks exon 29, resulting in a 19 amino acid deletion in the extracellular loop linking transmembrane helix IVS3 and IVS4. Using quantitative RT-PCR, this splice variant accounts for about 70% of CaV1.1 mRNA in cultured mouse myotubes. To characterize its biophysical properties, we deleted exon 29 in the rabbit α_{1S} subunit and expressed the resulting CaV1.1-ΔE29 in dysgenic (α_{1S}-null) myotubes. This channel variant supported skeletal muscle type EC coupling, but showed very distinct current properties. The amplitude was 8x higher than that of wild type CaV1.1 and the voltage-dependence of activation was left-shifted by 32 mV. The increased current amplitude was in part due to a 10-fold increased open probability. Current kinetics were accelerated by decreasing the time constant of the slow activation component, without reducing its relative contribution to the current. However, this effect did not involve the loss of interactions with the $\alpha_2\delta$-1 subunit, since siRNA depletion of $\alpha_2\delta$-1 caused an additional current acceleration by a different mechanism. Currently, CaV1.1-ΔE29 expression patterns in mammalian skeletal muscles are not known. However, its distinct current properties suggest that muscles expressing significant amounts of CaV1.1-ΔE29 will show distinct physiological EC coupling characteristics with an increased sensitivity to depolarization and a stronger contribution of Ca^{2+} influx to the cytoplasmic Ca^{2+} transients controlling contraction.

Support: FWF P17806-B05, P17807-B05, and the MCBO doctoral program W1101-B12.

3145-Pos Post-translational Modification Of LVA VDCC Subunits

Maureen W. McEnery, Anne Marie R. Yunker, Ya Chen, Alan H. Sharp

CWRU, Cleveland, OH, USA.

Board B448

Voltage-dependent Ca^{2+} channels (VDCC) are key mediators of Ca^{2+} influx, with low-voltage activated (LVA) VDCC implicated in early developmental processes as well as modulating cell excitability. Altered expression of LVA is implicated in several diseases including epilepsy and tumor differentiation. The family of LVA is comprised of three genes that give rise to Cav3.1/alpha1G, Cav3.2/alpha1H, and Cav3.3/alpha1I subunits. In this study, we explore the biochemical properties of native LVA (Cav3.1) expressed in adult rat brain and three recombinant LVA expressed in HEK293 cells taking guidance from the observation that the family of Ca_v3 alpha1 subunits is structurally similar to high-voltage activated (HVA) alpha1 as well as to alpha subunits of voltage-dependent sodium channel (VDSC). Using a panel of anti-LVA antibodies, we demonstrate for the first time that all three Cav3 subunit isoforms are glycosylated. The presence of N-linked glycosylation on recombinant and endogenous Cav3 isoforms was exploited to partially purify the proteins from detergent extracts. Following treatment with PNGase F the apparent mobility of each recombinant and endogenous protein is dramatically increased. In this way, LVA subunits are more similar to VDSC than HVA. A second distinguishing property of VDSC is the covalent attachment of beta2/beta4 subunits to the alpha subunit via a disulfide bond. Under conditions which clearly recapitulate the altered mobility of a VDSC alpha subunit following reductive alkylation, neither endogenous nor recombinant LVA subunits shift their apparent mobility suggesting there is no beta/beta4-like auxiliary subunit homolog. We suggest that inherited or acquired perturbations to the metabolic pathways that influence N-linked glycosylation of LVA alpha1

subunits or their association with auxiliary subunits may disturb the normal pattern of protein maturation of Ca_v3.

3146-Pos Beneficial Effects of Long-term Treatment with Beta-adrenergic Blocker on Depressed Heart Function of Female Rats

AYTAC A. SEYMEN, Erkan Tuncay, Hakan Gurdal, Belma Turan

health sciences, ankara, Turkey.

Board B449

Aging is the major risk factor for the development of cardiovascular diseases, the leading cause of morbidity, mortality and disability. On the other hand, it has long been recognized that incidence and prevalence of certain diseases vary with sex. Differences exist between women and men in the impact of risk factors, symptoms and therapeutic responses. Aging itself is also associated with down-regulation of beta-1 adrenoceptors. The use of beta-adrenergic blockers is now well established in the treatment of mild and moderate systolic heart failure. In this study, we examined the long-term effects of non-selective β-adrenoceptor blockers, timolol (5 mg/kg/day, n=10, intragastrically, 8 months) treatment, on hemodynamic and intracellular action potential parameters of heart from female rats. Significant depression (38%) in left ventricular developed pressure (LVDP), marked prolongations (73% and 51%) in two late-repolarization phases of action potential duration (APD_{75} and APD_{90}), and significant inhibition of L-type Ca^{2+}-current (47%) without any change in cell capacitance were observed in 9 mo old rats (n=27) compared to those of 3 mo old rats (n=30). Timolol administration caused a complete and a partial restoration of the depressed LVDP and the prolonged action potential duration in 9 mo old rat heart compared to those of 3 mo old rat heart, respectively. Timolol treatment also completely restored the depressed L-type Ca^{2+}-current in isolated left ventricular cardiomyocytes from 9 mo old rat heart. Our results suggest that timolol improved left ventricular function due to its beneficial effect on Ca^{2+}-influx in maturation- and/or aging-induced depressed cardiac function.

Supported by projects TUBITAK-PIA-10 & Ankara Univ BAP20060809233

3147-Pos Predicting Calcium Coordination in Calcium-Binding Proteins of Known Structure and L-type Calcium Channel

Ricky C. Cheng, Boris S. Zhorov

McMaster University, Hamilton, ON, Canada.

Board B450

Reproducing Ca^{2+}-protein complexes with flexible sidechains remains a problem. We elaborated a two-stage protocol that employs ZMM program, AMBER force field, implicit solvent, and distance- and environment-dependent dielectric function. At the first stage, tens of thousands starting points are generated with sidechain conformations and Ca^{2+} positions randomized in a 1000-$Å^3$ cube centered at the known Ca^{2+} position. Each starting point is optimized in a short Monte Carlo-minimization (MCM) trajectory. At the second stage, structures within 200 kcal/mol from the apparent global minimum are refined in long MCM trajectories. The protocol was tested in fourteen known Ca^{2+} binding sites including Ca^{2+} ATPase. In twelve cases, the RMSD of the apparent global minimum from the X-ray structure was < 2 Å. The two outliers were in proteinase K, in which Ca^{2+} solvation shells contain more waters than in other tested proteins. The protocol was used to predict Ca^{2+} chelation in the outer pore of L-type Ca^{2+} channel. The P-loop domain was folded as in $Na_v1.4$ (Tikhonov and Zhorov, Biophys. J., 2005). Two Ca^{2+} ions were loaded to counterbalance four ionized glutamates in the selectivity filter. Other ionizable residues were kept neutral. At the first stage, each Ca^{2+} ion was constrained to a pair of glutamates, but no constraints were used at the refinement stage. Several Ca^{2+}-chelating patterns were found with Ca^{2+} ions bound to two or more glutamates and the inter-ion axis being approximately parallel or perpendicular to the pore axis. In one complex, a Ca^{2+} ion occupied the level corresponding to potassium ion octacoordinated by Thr residues in the selectivity filter of K^+ channels. At this level, the Ca^{2+} ion is reachable by nucleophilic groups of ligands bound in the inner pore.

Supported by CIHR.

3147.01-Pos Optimization of recombinant $Ca_v2.2$ cell lines for drug screening

Janette Mezeyova[1], Xinpo Jiang[1], Afsheen Khawaja[1], Andrea N. Larsen[1], Johnny K. Lam[1], Elizabeth W. Tringham[1], Francesco Belardetti[1], Terrance P. Snutch[1,2], Stephen P. Arneric[1], David B. Parker[1]

[1] *Neuromed Pharmaceuticals Ltd., Vancouver, BC, Canada,*
[2] *Michael Smith Laboratories, UBC, Vancouver, BC, Canada.*

Board B450.01

$Ca_v2.2$ calcium channel blockers represent a promising class of analgesic for the treatment of chronic pain. (T.Snutch, NeuroRx. *2*: 662–70, 2005). Consequently, establishing an efficient *in vitro* functional screening assay is essential to identify novel small molecule $Ca_v2.2$ channel antagonists. While recombinant stable cell lines expressing $Ca_v2.2$ channels play an integral part of screening for novel compounds, we have found that constitutive expression of these channels in HEK293 cells leads to cell toxicity and inconsistent channel expression. We hypothesize that this is due to Ca^{2+} excitotoxicity caused by a tonic Ca^{2+} "window" current. Here we present an inducible $Ca_v2.2$ stable cell line with improved screening properties, generated using a tetracycline-regulated rat $Ca_v2.2$ subunit expression system together with constitutively expressed rat $\alpha_2\delta$-2 and rat β_{1B} subunits. Using 5 mM Ba^{2+} as the charge carrier, we obtained a mean peak current density of $-24.1 \pm$

8.1 pA pF^{-1} (n = 8) after 24 hours induction with 1.5 μg/ml tetracycline and, which remained stable up to 72 hours. The mean current density in sham-tetracycline induced cells was -0.39 ± 1.2 $pApF^{-1}$ (n = 24) in 72 hours, demonstrating the tight control of expression in the inducible system. Analysis of the biophysical and pharmacological properties of the exogenous $Ca_v2.2$ channels revealed that the properties were comparable to native N-type currents. The IC_{50} for the $Ca_v2.2$ blocker, -conotoxin GVIA was 18.9 ± 2.8 nM and a fit of the mean data with a Boltzmann function revealed parameters for steady-state activation of $V_{1/2} = -2.6 \pm 0.1$ mV (n = 6), $Vh_{1/2}= -43.3 \pm 1.4$ mV (n = 7) for steady-state inactivation.. The utilization of this cell line on an automated patch-clamp system will also be discussed. *J. Mezeyova and X. Jiang contributed equally to the project

Neuronal Systems & Modeling

3148-Pos Strong Adhesion Identifies Potential Neurite Extension And Polarization Sites In PC12 Cells

Leann L. Matta, Helim Aranda-Espinoza

University of Maryland, College Park, MD, USA.

Board B451

The dynamic process of neuronal polarization involves the development of neurites into an axon and dendrites. Important intracellular mechanisms have been identified during this process, including actin assembly and disassembly in the growth cone, microtubule dynamics, and cellular tension. It has been suggested that these mechanisms may play a role in axonal specification; however, little attention has been placed on cell spreading and adhesion occurring prior to neurite extension. Here we begin to describe the role of strong adhesion and spreading during the initial polarization stages for PC12 cells, which in the presence of neurotrophic factors, are capable of differentiating into sympathetic-like neurons. We evaluated initial attachment, cell-substrate adhesion, and spreading dynamics of PC12 cells on collagen coated substrates using Interference Reflection Microscopy, and developed an image process algorithm to measure cell spreading area and strong adhesion zones during initial neurite outgrowth. A correlation between zones of adhesion and neurite development was identified to occur in three different stages during the first 90 minutes of spreading. The first stage occurs during initial spreading before neurites have developed, and when zones of adhesion are localized within the cell body. Spreading boundaries reveal anisotropic growth, with a rate of growth of 0.26 (micron2/min) during this early stage. Total spreading area continues to increase during stage two, with a similar speed. Neurites begin to develop and a competition effect is observed, where strong adhesion occurs at multiple neurite anchoring sites. The level of adhesion appears to specify which neurite develops versus those which retract. In stage three, maximum spreading area is achieved, and polarization appears to begin, with strong adhesion localized at the site of polarization. This data suggests an importance in adhesion dynamics during both neuronal spreading and polarization.

3149-Pos Live Imaging of Neural Differentiation in the Developing Brain Using 2-Photon Laser Scanning Microscopy

Nicolas FRITZ, Per Uhlén

Karolinska Institutet, Stockholm, Sweden.

Board B452

During cortical development, neural migration and differentiation are precisely regulated by complex signaling cascades. To further our understanding of these essential mechanisms for embryonic cortical development we have to monitor these signaling events in the living brain. We performed live-imaging studies of neural progenitor migration/differentiation and calcium (Ca^{2+}) signaling in the embryonic neocortical environment. Using high-end customized 2-photon laser scanning microscopy, we examined these deep-tissue cellular events in brain slices from transgenic mouse strains expressing GFP under the promoter of the differentiation stage-specific markers GFAP (Glial Acidic Fibrillary Protein) and tau.

Our results show that GFAP-expressing neural progenitors are dividing in the subventricular zone and migrate radially towards the pia whereas tau-expressing cells migrate mostly tangentially. GFAP-expressing cells are mainly located in the ventricular and subventricular zones whereas the tau-expressing cells are more diversely spread. Moreover, intracellular Ca^{2+} recordings point towards a Ca^{2+} signaling-dependency of these critical differentiation and migration processes. In summary, here we show distinct neural migration patterns of neural progenitors and neurons in the embryonic neocortical environment of the living brain which are crucial for the establishment of the cortical architecture during embryonic development.

3150-Pos A Computational Approach Describing The Distinct Effects Of Topographical Versus Chemical Cues On Axogenesis

Leandro Forciniti

University of Texas-Austin, Austin, TX, USA.

Board B453

Understanding how external cellular cues affect axogenesis, the formation of an axon in neurons, is a necessity for the development of novel scaffolds for nerve repair. Of particular interest is the distinct behavior Hippocampal neurons exhibit when comparing topographical cues to immobilized chemical cues (i.e. Neural Growth Factor). In order to further understand this behavior a two fold approach involving computation modeling and experiments was employed. Assuming that the decisive factor between these cues is an effective surface concentration of cues, our model successfully described previous neuronal behavior seen by Gomez et al as well as made predictions that were then tested experimentally. The model considers the following factors: excluded volume of the growing neurites as well as the cell soma, number of initial